

REMOTE SOUNDING OF THE EARTH'S ATMOSPHERIC LIMB FROM A MICRO-SATELLITE PLATFORM: A FEASIBILITY STUDY OF THE ALTIUS MISSION

D. Vrancken⁽¹⁾, B. Paijmans⁽¹⁾, D. Fussen⁽²⁾, E. Neefs⁽²⁾, N. Loodts⁽²⁾, E. Dekemper⁽²⁾, F. Vanhellefont⁽²⁾,
L. Devos⁽³⁾, W. Moelans⁽³⁾, D. Nevejans⁽⁴⁾, H. Schroeven-Deceuninck⁽⁵⁾, D. Bernaerts⁽⁵⁾, J. Zender⁽⁵⁾

⁽¹⁾Verhaert Space, Hogenakkerhoekstraat 9, 9150 Kruibeke, Belgium, e-mail: Davy.Vrancken@verhaertspace.com

⁽²⁾BIRA/IASB, Ringlaan 3, 1180 Brussels, Belgium, e-mail: Didier@oma.be

⁽³⁾OIP, Westerring 21, 9700 Oudenaarde, Belgium, e-mail: ldv@oip.be

⁽⁴⁾Conserd, Krekelstraat 27, 9052 Gent, Belgium, e-mail: Dennis.Nevjans@conserd.net

⁽⁵⁾ESA/ESTEC, Keplerlaan 1, 2201 AG Noordwijk, The Netherlands, e-mail: Hilde.Schroeven-Deceuninck@esa.int

ABSTRACT

There is more and more interest in the understanding and the monitoring of the physics and chemistry of the Earth's atmosphere and its impact on the climate change. Currently a significantly high number of sounders provide the required data to monitor the changes in atmosphere composition, but a dramatic drop in operational atmosphere monitoring missions is expected around 2010. This drop is mainly visible in sounders capable of a high vertical resolution. Currently, instruments on ENVISAT and METOP provide relevant data but this is envisaged to be insufficient to ensure full spatial and temporal coverage and redundancy in the measurement data set.

ALTIUS (Atmospheric Limb Tracker for the Investigation of the Upcoming Stratosphere) is a remote sounding experiment proposed by the Belgian Institute for Space Aeronomy (BIRA/IASB) for which a feasibility study was initiated with BELSPO (Belgian Science Policy) and ESA support. The main objective of this study phase was to establish a mission concept, to define the required payload and to establish a satellite platform design. The study was led by the BIRA/IASB team and performed in close collaboration with OIP (payload developer) and Verhaert Space (spacecraft developer).

The mission scenario includes bright limb observations in basically all directions, solar occultations around the terminator passages and star occultations during eclipse. These observation modes allow imaging the atmosphere with a high vertical resolution. The spacecraft will be operated in a 10:00 sun-synchronous orbit at an altitude of 695 km, allowing a 3-day revisit time.

The envisaged payload for the ALTIUS mission is an imaging spectrometer, observing in the UV, the VIS and the NIR spectral ranges. For each spectral range, an AOTF (Acousto-Optical Tunable Filter) will permit to perform observations of selectable small wavelength

domains. A typical set of 10 wavelengths will be recorded within 1 second.

The different operational modes impose a high agility capability on the platform. Furthermore, the quasi-continuous monitoring by the payload will drive the design of the platform in terms of power and downlink capabilities. The mission will be performed using a derivative of the PROBA platform, developed by Verhaert Space.

This paper will present the mission requirements for the ALTIUS mission, the envisaged instrument, the spacecraft concept design and the related mission analysis.

1. INTRODUCTION

The work presented in this paper is the output of a phase A study, performed for ESA (European Space Agency) under a Prodex contract.

A study has been performed, compiling past, present and future atmospheric missions. This study [10] shows a potential issue in the monitoring of the Earth's atmosphere with a global coverage (Fig 1).

Clearly, the number of available sounders will drop dramatically and this is particularly true for space instruments having a high vertical resolution. Furthermore, during the period 2005-2006, four very important and successful missions were lost or switched off: SAGE II, SAGE III, POAM and HALOE. Not only this loss of instruments is detrimental for pure atmospheric research (all together these four instruments capitalize 47 cumulated years of measurements and about 4800 scientific papers) but it has dramatic consequences on the monitoring of long-term trends for essential atmospheric species like ozone or water vapor.

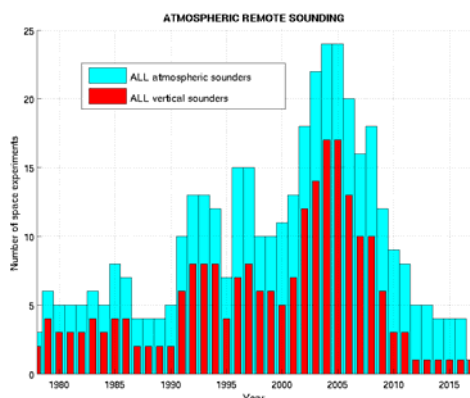


Figure 1: Dramatic decrease of atmospheric sounders between 2006 and 2010

There remain a few instruments working on ENVISAT and SCISAT. Also some new sounders are now active (e.g. on METOP) but this is insufficient to ensure a full spatial and temporal coverage as well as a minimal redundancy in the measurement data set.

Some nadir-looking instruments of the GOME type possess a high horizontal resolution well suited for pollution detection and monitoring but at the price of a poor vertical resolution, not compatible with the refinement of modern CTM modeling codes. A correct understanding of the stratospheric chemistry requires ideally a 1 km vertical resolution, whereas a horizontal resolution of about 300 km, typical for occultation instruments, is acceptable. The ALTIUS mission will be designed to meet these requirements.

The proposed payload for the ALTIUS mission is an imaging spectrometer, operating in the UV, VIS and NIR. Each spectral channel is equipped with an AOTF (Acousto-optical Tunable Filter) to select a narrow spectral band from the incoming light.

Due to the tight budget and schedule constraints, a PROBA-like platform has been selected for the mission. The PROBA satellite is a small satellite that was developed by Verhaert Space for ESA. The proposed platform is based on the PROBA-2 spacecraft, with modifications to the structure, the AOCS subsystem and the implementation of an X-band downlink system. The small satellite approach has its inherent limitations. The main constraint, imposed by the platform onto the mission is the amount of incoming power, which limits the amount of data that can be gathered and downlinked per orbit. However, the performance that can be achieved with the platform provides a sufficient data set for the scientists.

2. ALTIUS SCIENTIFIC CONTEXT

There is an increasing interest in the understanding and the monitoring of the physics and the chemistry of the troposphere due to their potential importance for the human beings. Yet, the evolution of the climate is fundamentally driven by the entire atmosphere through its global transport properties, its chemical composition and its interaction with the solar radiation.

It is now accepted that the global and polar depletions of the ozone layer can be attributed to the presence of halogen compounds released by anthropogenic emissions. The Montreal protocol has allowed observing a decrease in the stratospheric halogen load and a slowing of ozone decline is expected to be the natural precursor of a complete ozone recovery around the mid-century. There is presently experimental evidence that the global mean ozone total column is no longer decreasing with respect to the 1998-2001 period. Also, the ozone stratospheric distribution has been relatively constant during the last decade although both dynamical and chemical processes may contribute to decadal changes in the lower stratosphere. On the other hand, column ozone loss in the 2004/2005 Arctic winter was among the largest ever observed whereas Antarctic ozone depletion has probably stabilized during the last decade.

Clearly, the monitoring of ozone stratospheric abundances is of crucial importance in assessing the milestones of a clear recovery process.

Among important trace gases, methane is very important for its impact on climate through a large radiative forcing effect and the production of stratospheric water vapor. A global increase of about 0.7 ppm in 1800 AD to 1.8 ppm nowadays is difficult to interpret because of the diversity of the sources: wetlands, enteric fermentation, fires and rice agriculture.

The odd hydrogen family, HO_x, contains all active species, i.e. radicals that are involved in catalytic cycles that destroy O₃. The HO_x radicals are derived primarily from the oxidation of water vapor in the stratosphere and therefore it is essential to understand and to monitor the intrusion of water vapor into the stratosphere, specially in the region of the tropical tropopause.

Similarly, the NO_x family is known to play an essential catalytic role in ozone destruction with a strong diurnal cycle that requires day- and nighttime measurements for a full characterization. On the other hand, these species may be converted into inactive forms or reservoirs. In particular, the NO₂ reacts with ClO to form ClONO₂ and the measurement of OCIO (depending itself from the presence of ClO and BrO) and BrO (daytime) in the

UV is very important if it can be anti-correlated with NO₂ simultaneous observations.

The role of polar stratospheric clouds (PSCs) in polar ozone depletion has been described extensively in scientific literature ([13]). Briefly, in cold conditions, when PSCs are present, the stable reservoir species HCl, ClONO₂ and N₂O₅ disappear in heterogeneous reactions on the surface of the particles to form HNO₃ inside the PSC particles, which are eventually removed from the stratosphere by sedimentation in a process called de-nitrification. The other reaction products are photo-dissociated in the presence of sunlight (at the end of polar winter, when the Sun returns) to chlorine species, which act as catalytic ozone scavengers.

Much remains to be learned about PSCs. The current classification is probably too coarse. We do not know enough about particle sizes, crystal morphology and even composition. On a larger scale, more information is needed about cloud properties such as shape, thickness and density. Satellite measurements can provide this information: PSCs are easily recognized when elevated optical extinctions are observed inside the polar vortex.

Polar mesospheric clouds (PMCs), originally called noctilucent clouds, are (as the name suggests) only visible in the dark sky, long after sunset. PMCs were reported for the first time in 1885. They are similar in appearance to thin cirrus clouds, but are located at the much higher altitudes from 80 to 87 km, near the mesopause. PMCs only occur at high latitudes during summer (a few weeks before and after the solstice), when the mesosphere becomes extremely cold (with temperatures even as low as 100 Kelvin). Various pieces of evidence, including direct rocket sampling, suggest that they are composed of very small water-ice particles (0.05 – 0.1 μm).

According to the IGACO report ([11]), which was taken as a scientific reference for the phase A study, it is necessary to obtain a comprehensive set of global observations of the species quoted in Table 1 for the stratosphere by using LEO satellites. In addition to the needs expressed in the IGACO report, there are also atmospheric modeling capabilities which embark on the creation of a global picture in the combination of these atmospheric data.

It is highly desirable to combine the advantages of nadir-viewing and limb-viewing techniques. What is ideally needed is an instrument with a vertical resolution similar to that of an occultation instrument but with coverage similar to that of a backscatter instrument.

Table 1: Observation needs following IGACO

| Atmospheric Region | Requirement | Unit | O ₃ | NO ₂ | CH ₄ | H ₂ O | CO ₂ | BrO | Aerosols |
|--------------------------------------|-------------|------|----------------|-----------------|-----------------|------------------|-----------------|-------|----------|
| 3. Lower stratosphere | Dx | km | 100 | 250 | 250 | 200 | 500 | 100 | 100 |
| | Dz | km | 3 | 4 | 4 | 3 | 4 | 1 | 1 |
| | Dt | | 1d | 12hr | 12hr | 1d | 1d | 6h | 1w |
| | Total error | % | 20 | 40 | 30 | 20 | 2 | 15 | - |
| | delay | | weeks | hours | weeks | weeks | months | weeks | weeks |
| 4. Upper stratosphere, mesosphere | Dx | km | 200 | 250 | 250 | 200 | 500 | 100 | - |
| | Dz | km | 3 | 4 | 4 | 5 | 4 | 1 | - |
| | Dt | | 1d | 1d | 1d | 1d | 1d | 1d | - |
| | Total error | % | 20 | 40 | 30 | 20 | 2 | 20 | - |
| | delay | | weeks | weeks | weeks | weeks | months | weeks | - |

Since the pioneering work of the SOLSE/LORE experiment ([1]), it has been established that the limb scattering technique is a viable technique for the measurement of atmospheric trace gas profiles in the stratosphere. A confirmation of this approach has been recently published for OSIRIS on board ODIN ([2]), for SCIAMACHY on board ENVISAT ([3]) and for the SAGE III mission before its premature end ([4]).

All the above-mentioned experiments have measured and validated ozone and NO₂ profile retrievals and their results concerning BrO, OClO and aerosols will be published in forthcoming scientific papers. Also, the limb scattered light recorded by the upper and lower bands of the GOMOS detector (on board ENVISAT) is presently investigated in order to develop an inversion algorithm.

However, it is now recognized that the limb scattering technique suffers from a major difficulty associated with the difficulty of an accurate determination of the tangent altitude associated with a particular line-of-sight because of the diffuse nature of the light source ([5]).

ALTIUS will also make use of the limb scattering technique but its imaging capacity will allow solving the issues of altitude registration, cloud identification and horizontal gradients of measured species.

It should be taken into account that any measurement toward the limb (scattering or occultation) leads to an effective path length along the line-of-sight of about 500 km. Perpendicular to the line-of-sight and parallel to the horizon, the spatial resolution shall be mainly limited by the number of pixels needed to obtain the necessary S/N ratio imposed by the inversion algorithm. Finally, the vertical resolution shall be equal or better than 1 km.

3. ALTIUS MISSION REQUIREMENTS

The ALTIUS mission requirements for the target atmospheric species are summarized in Table 2 with a particular focus on vertical resolution. The table

considers the priority of data collection. The dark-shaded rows concern global ozone [priority 1] whereas the light-shaded rows [priority 2] refer to species explicitly mentioned in the IGACO requirement table (Table 1). The other species [priority 3] are mentioned in experimental "demonstration" mode.

Table 2: ALTIUS target atmospheric species

| | z [km] | A [%] | λ [nm] | bright limb | occultation | Dx,Dy,Dz [km] | Full coverage |
|------------------|--------|-------|-----------------|-------------|-------------|---------------|---------------|
| O ₃ | 10-30 | 5 | 550-650 | x | x | 500,10,1 | 3d |
| O ₃ | 30-50 | 5 | 300-350/550-650 | x | x | 500,10,1 | 3d |
| O ₃ | 50-100 | 20 | 250-300 | | x | 500,NA,1 | 3d |
| NO ₂ | 20-50 | 30 | 450-550 | x | x | 500,20,2 | 3d |
| CH ₄ | 5-25 | 20 | 1600-1800 | x | x | 500,50,2 | 3d |
| H ₂ O | 10-30 | 20 | 900-1800 | x | x | 500,50,2 | 3d |
| CO ₂ | 10-30 | 20 | 1550-1600 | x | x | 500,50,2 | 3d |
| BrO | 10-30 | 20 | 320-360 | x | | 500,50,1 | 3d |
| OCIO | 15-50 | 25 | 320-400 | | x | 500,50,1 | 3d |
| NO ₃ | 20-50 | 25 | 662 | | x | 500,50,1 | 3d |
| aerosols-PSC | 10-30 | 25 | 200-2000 | x | x | 500,20,1 | 3d/1 y |
| O ₂ | 60-100 | 30 | 1260-1270/1530 | | x emission | 500,100,5 | 3d |
| PMC | 70-100 | 50 | 200-2000 | x | x | 500,20,1 | 1 y |

The primary scientific target of the ALTIUS mission will be the measurement of the ozone concentration vertical profiles. This concentration should be retrieved with accuracy of 5 % between 10 and 50 km, and of 20 % between 50 km and 100 km. The optimal ozone measurements will be performed around 550-650 nm (Chappuis band) in the lower stratosphere, around 320-350 nm (Huggins band) in the upper stratosphere and 230-270 nm (Hartley band) in the mesosphere in occultation mode only. The instrument has to be able to measure ozone in the polar night as well as at different local times in the mesosphere (in particular around the second ozone maximum).

Global coverage has to be performed in a delay equal or less than 3 days to offer continuity with respect to ENVISAT atmospheric instruments, with a resolution of 5 degrees in latitude and 10 degrees in longitude, a threshold requirement for the accuracy of present chemical assimilation models.

The ALTIUS instrument will use the hypercube measuring technique in a limb viewing geometry. Instead of a traditional "spatial x (spatial x wavelength)" construction an innovative "(spatial x spatial) x wavelength" approach will be adopted. Therefore ALTIUS will be a spectral camera with wavelength scanning. This approach will allow solving, in a definitive way, the altitude registration problem that is spoiling the traditional limb scatter technique.

The ALTIUS instrument shall be basically an imager with the limb itself as scope (Figure 2). The field-of-view of the instrument (an extended scene of the sounded atmospheric region has to be aimed for) will cover the entire atmospheric limb, hence different solutions will exist to improve the classical (and unsatisfactory) method of total radiance fitting in the UV ("Knee"-methods – (1)), such as using: the horizon or geographical details in cloudless scenes (2), background stars in the scene (3) and satellite star tracker information (4).

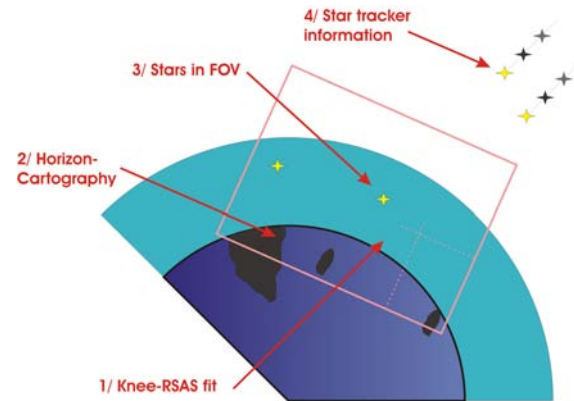


Figure 2: Illustration of the ALTIUS concept. The attitude registration is performed by the combination of the star tracker information, the position of stars in FOV and geographic features

4. MISSION ARCHITECTURE

A sun-synchronous orbit with an altitude of 668.5 km and a local time of 10:00 has been chosen for the ALTIUS mission. This orbit allows for a revisit time of exactly 3 days.

In the baseline mission concept, no orbit corrections are envisaged during the course of the mission. The lack of orbit maintenance will result in a drift of the local time over the envisaged 5 years mission time. The drift has not been identified as a killer from science point of view, but will result in problems on the spacecraft towards the end of the mission. The problems are related to the reduced incoming power or star tracker blinding, depending on the direction the spacecraft is drifting (depending on the chosen inclination and the orbit injection errors from the launcher).

Due to the lack of an orbit control system, no end-of-life disposal is envisaged. The end-of-life disposal has not been introduced as a hard requirement, but might be imposed to the mission in the (near) future. When a propulsion system will be incorporated for the de-orbiting, it will also be used for the orbit maintenance during the 5 years mission.

The ALTIUS mission has been designed towards an operational phase, which will use only the Redu ground station (5.15°E, 50.00°N). The Redu ground station will have to be equipped with a 3m receiving X-band antenna. The average contact time per day for this ground station is 34.5 minutes, which is sufficient to downlink all the collected science and housekeeping data.

5. PLATFORM

The ALTIUS spacecraft will be based on the bus of the PROBA2 satellite. Most of the bus elements can be reused, which will minimize the development time and risk and will result in a cost effective solution.

The spacecraft concept for ALTIUS is shown in Figure 3. The solar panel is deployed 140° to optimise the amount of incoming power. In nominal operational mode, the camera will be backward looking, i.e. in the anti-velocity direction and tilted 64.38° around the pitch axis with respect to nadir.

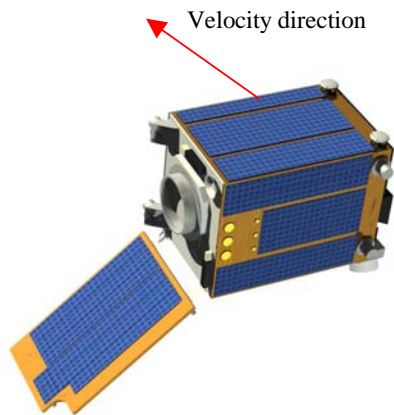


Figure 3: ALTIUS spacecraft concept

5.1. Structure

The satellite structure is made from honeycomb panels with Carbon Fiber Reinforced Plastic (CFRP) face sheets. The inner structure, which holds all the bus units and the payload, consists of 2 parallel panels. The size of the payload does not allow incorporating a full structural panel between these 2 panels, as was the case for PROBA-1 and PROBA-2. Only a small supporting structure can be implemented in between the internal structural panels. To cope with this, the bottom board needs to be stiffened to obtain a satisfactory first eigenfrequency of the spacecraft.

Four solar panels are body-mounted and are part of the primary structure, contributing to the overall stiffness of

the spacecraft. An additional deployable solar panel is mounted on the satellite.

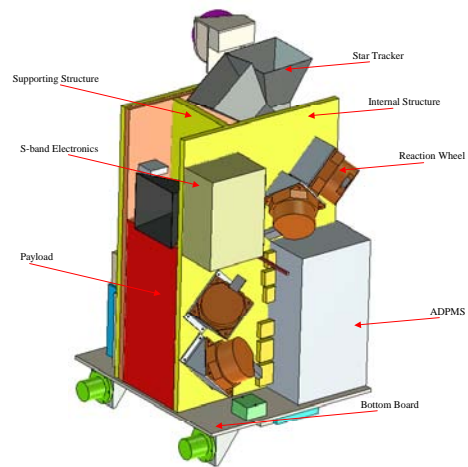


Figure 4: Internal accommodation of the ALTIUS spacecraft

The size of the spacecraft is 810 mm x 630 mm x 640 mm and its weighs 133 kg. Figure 4 gives a view of the interior of the ALTIUS spacecraft. The 3 star trackers are mounted on the optical bench of the payload. The payload itself is mounted isostatically to the internal structure. A view on the outer structure is given in Figure 5.

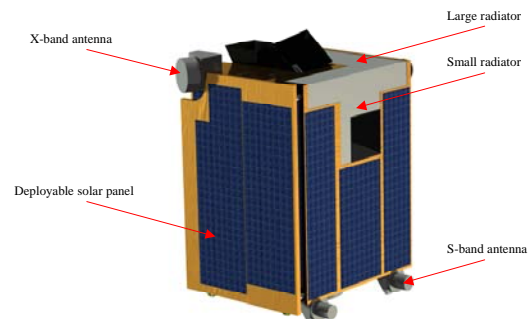


Figure 5: External accommodation with solar panel in stowed configuration

5.2. Avionics

The onboard computer and data handling system for the ALTIUS mission is based on the ADPMS (Advanced Data and Power Management System), which is fault-tolerant computer and power system of PROBA2 and developed by Verhaert Space for ESA.

ADPMS consists of two main parts: a Data Management Unit (DMS) and a Power Management System (PMS). The DMS is a powerful computer built on Compact PCI (cPCI) modules around the LEON2 processor. Primary and Redundant PCI lanes form a fault-tolerant architecture. The LEON2 (Atmel AT697F) provides a capacity of 86 MIPs or 23 MFLOPS. The PMS is based on an unregulated battery bus architecture capable of delivering up to 300W in total on 24 outputs that are each limited to 50W.

The DMS provides data handling for all subsystems and control for the space segment. This also involves the execution of attitude control maneuvers either in response to ground command or using on-board algorithms, and the execution of all on-board autonomy related functions.

ADPMS provides up to 25 RS-422 and two PacketWire interfaces, although the design can be easily adapted for other standards (CAN, SpaceWire, MIL-STD-1553). ADPMS also provides 8 programmable channels for clock distribution and 3 channels for datation input, mainly to synchronize the ADPMS clock with the GPS PPS. The 12Gbit of on-board data storage required by the payload are provided by the MCPM (Mass Memory Payload Module) of ADPMS. The Front End Electronics (FEE) of the payload will interface ADPMS through PacketWire. Telemetry and Telecommand are implemented according to CCSDS standards.

The electrical architecture, as shown in Figure 6, is built-up around the ADPMS. Each subsystem in the block diagram is described in the next sections.

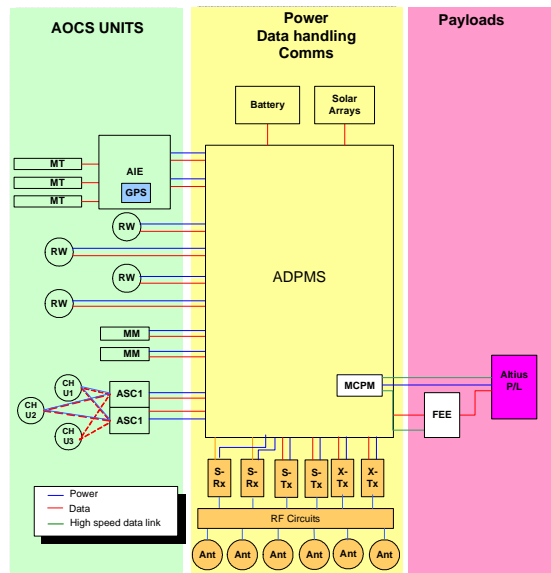


Figure 6: ALTIUS S/C electrical architecture

5.3. AOCS

The ALTIUS satellite is three-axis stabilized. The attitude measurements are done by:

- Three autonomous **star trackers** (hot-redundant optical heads and one cold redundant star tracker electronics)
- Four **Reaction Wheels**, which are mounted in a tetrahedral configuration.
- A cold-redundant **GPS receiver** and two **antennas** provide the essential orbital position, velocity and correlation to a universal time reference.
- Three **magneto-torquers** are mounted in three orthogonal directions. The torquers will be used to offload wheel momentum. The magneto-torquers are dual wound and are therefore internally redundant.
- Two cold-redundant **magnetometers** to measure the magnetic field of the Earth

The ALTIUS AOCS Software (SW) will be an update of the PROBA AOCS SW and has the following modes:

- **Safe mode**
The safe mode is based on the Bdot algorithm. It uses the magnetometers as sensors and the magnetic torquers as actuators. The algorithm will reduce the spacecraft rotational speed to twice the spacecraft orbital rate. This mode is used as safe mode, but also to detumble the spacecraft after separation.

- **Observation mode.**
Different observation modes are defined:
 - In the nadir pointing mode, the payload is pointed towards the Earth's centre and the satellites bottom board is oriented towards the negative Pitch axis of the orbit;
 - The backward pointing mode is performed starting from Nadir followed by a rotation around the Pitch axis of -64.38° (angle between Earth's centre and bright limb). This is the orientation during the baseline operational scenario. In this attitude, the primary X-band antenna is pointed towards nadir.
 - The forward pointing mode is performed starting from Nadir followed by a rotation around the Pitch axis of 64.38° (angle between Earth's centre and bright limb); in comparison with the previous two attitudes, the detector of the payload is rotated 180° around the line of sight;

- The left pointing mode is performed starting from backward looking followed by a rotation around the Yaw-axis of the orbit of $+90^\circ$. There remains a single star tracker coverage until a rotation of $+130^\circ$, which is useful for a tomography scenario. If the left pointing mode is performed starting from forward looking, there is a single star tracker coverage until Yaw-rotations of -40° .
- A partially right pointing mode can be performed starting from backward looking followed by a rotation around the Yaw-axis of -45° .
- The dark sky pointing mode can be performed starting from backward pointing followed by a rotation around the Pitch axis of -4° till -6° .
- A star occultation mode starts from an attitude similar to the dark sky pointing (= payload pointing 4° to 6° above the atmosphere. Once a star is acquired by the payload, the spacecraft will go into inertial pointing mode, until the star has set behind the Earth.
- The Sun occultation mode uses the same orientation as for backward pointing (for sun set (SS)) or forward pointing (sun rise (SR)).

- **Sun-bathing mode**

This is a 3-axis stabilised mode, keeping the solar arrays optimally pointed to the sun in order to maximize the incoming power.

The nominal missions scenario is shown in Figure 7.

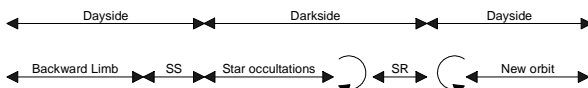


Figure 7: Nominal mission scenario

In the bright limb, the spacecraft is oriented in backward looking mode. When going into eclipse a sun occultation observation is performed. In eclipse, a number of star occultations are performed. Just before reaching the terminator, the spacecraft is oriented in forward looking mode to perform a sun occultation during sunrise. Before resuming the bright limb observations that spacecraft is again oriented in backward looking mode.

A tomography scenario is composed of at least 2 orbits (see Figure 8). A standard backward looking orbit in the bright limb, is followed by a left looking orbit. Due to fact that the angular distance to the side horizon is close

to the angle by which the Earth will have rotated at the next LEO revolution, it is possible to combine a backward limb observation followed by a dedicated sideward limb observation of the same location at the consecutive orbit.

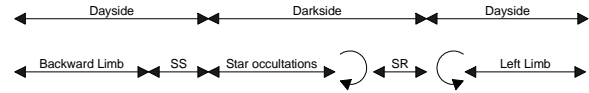


Figure 8: Tomography scenario

The main part of the ALTIUS AOCS SW can be re-used from PROBA-1 and PROBA-2.

5.4. Communication

The S-band receiver and transmitter from PROBA-2 are reused on the ALTIUS spacecraft. The S-band system incorporates a hot redundant receiver and a cold redundant transmitter. The S-band system will be used for commanding the spacecraft and for receiving the housekeeping data (in case the X-band system is not used). Four S-band antennas are incorporated to ensure an omni-directional coverage for the receivers.

The S-band system will be complemented by an X-band transmitter. The X-band electronics are cold redundant. 2 X-band antennas are incorporated onto the S/C; an isoflux antenna (for nominal use), with a wide angle, connected to the primary chain of the transmitter and a high-gain, narrow angle X-band antenna linked to the redundant channel (as back-up). Since the high gain antenna is mounted on the bottom board of the spacecraft, the satellite must be re-oriented during transmission, which means that the observations have to be interrupted. In order to avoid a systematic gap in the obtained data set above a certain region, a back-up ground station in St-Hubert (Canada) has been identified. In case of an anomaly with the primary downlink system, the 2 ground stations can be used in an alternating way. A high gain antenna has been selected in the redundant downlink chain to minimize the science data downlink time, and as such the gap in the data set.

The total amount of science data, gathered during 1 orbit is equal to 1.86 Gbits. A downlink rate of 15 Mbps is chosen. A positive link budget is obtained, assuming a 3 m antenna at Redu.

5.5. Power

The solar panel configuration for ALTIUS consists of four fixed body mounted panels and an additional hinged deployable. The latter will deploy over an angle

of 140°. It is a simple and compact design using the latest high efficiency triple-junction GaAs solar cells.

An 18 Ah Li-Ion battery is used to supports the eclipse periods and high power phases. A maximum Depth-Of-Discharge of 20 % has been assumed for the sizing of the battery.

The obtained power subsystem provides a 28 V unregulated power bus.

A positive power budget is obtained with the power subsystem in the nominal operational mode. The battery can fully recharge during the bright limb phase (see Figure 9).

In the off-nominal (scientific) modes, the incoming power profile is less favourable and the battery will not recharge completely. Therefore it is required to maintain the spacecraft in a sunbathing mode in the following orbit.

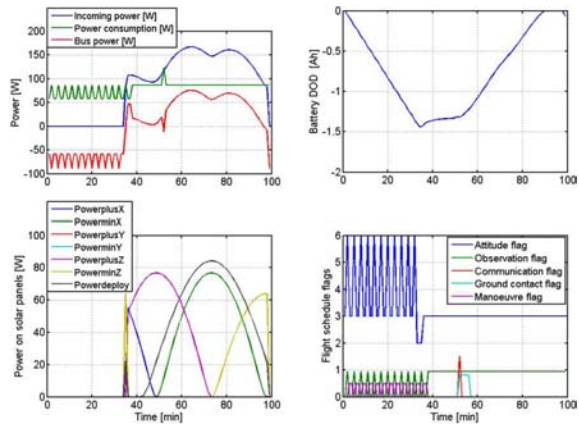


Figure 9: Power budget for baseline operational scenario

5.6. Thermal

A passive thermal control system has been incorporated, using mainly paint and MLI.

Special attention has been paid to the thermal control of the payload. The IR detector is actively cooled using a Sterling cooler. Since the cooler will dump the heat directly into the optical bench of the IR channel, the heat must be rejected as efficiently as possible. Also the IR optics must be maintained at a low temperature to reduce the contribution of the thermal background of this channel. For the VIS and UV channel the temperature of the optics is less critical, but the temperature of the detectors should be sufficiently low in order to reduce dark current.

Two radiators are incorporated onto the spacecraft. The radiators are directly linked to the optical bench of the IR channel and to the UV and VIS detectors. The complete IR optical bench is thermally isolated from the other channels using quartz spacers with a low thermal conductivity. The VIS and UV detectors are also thermally isolated and are connected to the IR optical bench using thermal straps. The relatively high mass of the optical bench stabilizes the temperature of all the thermally sensitive equipment.

In the worst case, the temperature of the IR optical bench reaches 2.6°C, which is low enough to guarantee the optical performance. The temperature of the VIS and UV detectors remain at a temperature of 11.6°C, which is allowable to maintain a low enough dark current.

6. PAYLOAD

6.1. General description

The payload for the ALTIUS mission is an imaging spectrometer that makes use of an Acousto-Optical Tunable Filter (AOTF) to select a narrow spectral band out of the incoming light.

The instrument basically consists of:

- front end optics that match the beam diameter and field angle of the incident light to the aperture and acceptance angle of the AOTF,
- the AOTF that is used to select the wavelength band,
- back end optics that image the observed scene on the detector array

Additional optics is needed to make the photon flux on the detector the same order of magnitude in the different viewing modes:

- a moveable ND filter can be brought into the light path to reduce the transmission during solar occultation observations
- an additional telescope reduces the FOV during stellar occultation observations. In this observation mode, the light is directed through the telescope by means of a moveable mirror and a shutter mechanism

A schematic representation of the optical system of the payload is given in Figure 10.

The instrument covers the spectral range between 250nm and 1800nm. As the working range of an AOTF is limited to typically one octave, three channels are needed to cover the total spectral range:

- UV channel from 200nm to 400nm,
- VIS channel from 400nm to 800nm and
- NIR channel from 800 to 1800nm.

The dimensions of the payload are 260x547x500mm³, its mass is around 35kg and the total power budget is 35W.

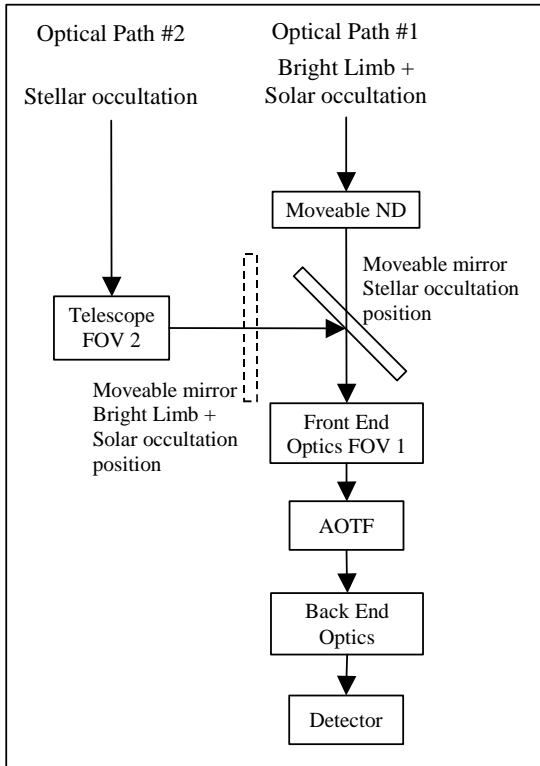


Figure 10: Schematic representation of the optical layout of the instrument

6.2. Optical system concept

For the optical system two different layout concepts can be used. They are schematically shown in Figure 11.

The most commonly used is the layout where the front end optics is an afocal telescope that images the entrance pupil of the optics on the aperture of the AOTF and that matches the FOV of the instrument to the acceptance angle of the AOTF. The back end optics is an objective that images the light leaving the AOTF on the detector.

Because the AOTF is essentially a diffraction grating, different wavelengths will be diffracted under slightly different angles. This results in the following major disadvantages of this concept:

- an image with a gradually changing wavelength.
- a blurring of the spot as a result of the AOTF bandwidth and consequently a loss of resolution [14].

These effects do not occur with an alternative layout, where the front end optics is a telecentric objective that images the scene on the aperture of the AOTF. In this concept, the numerical aperture of the objective is

matched to the acceptance angle of the AOTF. The back end optics is a relay system that transports the image to the detector and matches the size of image, i.e. the size of the AOTF aperture, to the size of the detector.

A better resolution can be obtained with this layout in the direction parallel to the plane of diffraction [15]. The disadvantage of using the second layout is that any defects in the AOTF crystal will be visible in the image.

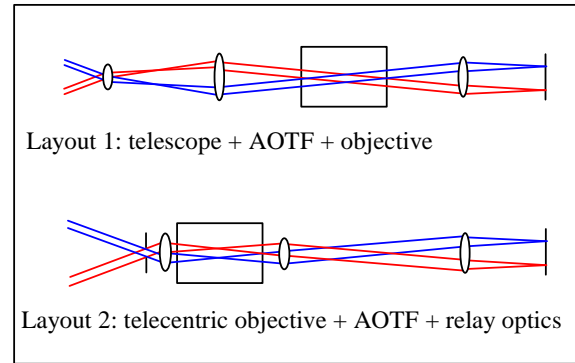


Figure 11: Schematic layouts for ALTIUS

6.3. Optical system description

The optics has to be matched to the aperture and acceptance angle of the AOTF, regardless of the chosen layout; therefore the AOTF will define the étendue of the system. For a given FOV, the entrance pupil diameter is defined by the AOTF.

Apart from increasing the bandwidth of the AOTF and optimizing the transmission of the optics, there are only limited possibilities to increase the photon flux on the detector.

In bright limb mode, where the light source is an extended source, the photon flux on a detector pixel can be increased by reducing the number of pixels over the FOV.

In stellar occultation mode the light source is essentially a point source. The photon flux on the detector will be proportional to the area of the entrance pupil which in its turn will be inversely proportional to the FOV squared.

The number of pixels in bright limb mode and the FOV in stellar occultation mode have been chosen so that the photon flux is optimized while at the same time the differences in the photon flux between both observation modes is minimized.

The parameters used in the design of the payload are given in Table 3. The FOV for bright limb observations (FOV1) corresponds to 300x300km² at a distance of 3000km in the visible channel and 100x100km² at a distance of 3000km in the two other spectral channels. All three channels have the same spatial resolution.

In the stellar occultation mode, the FOV is chosen so that the entrance pupil diameter is 50mm. This is the largest aperture that can be fitted in the volume available for the payload.

Table 3: Optical Parameters

| Parameter | UV | Visible | NIR |
|--------------------------------|-------------|------------------|------------------|
| Spectral band [nm] | 250 - 400 | 400 - 800 | 800 - 1800 |
| AOTF material | KDP | TeO ₂ | TeO ₂ |
| AOTF aperture [mm] | 5 x 5 | 10 x 10 | 10 x 10 |
| AOTF acceptance angle [°] | 2 | 5 | 5 |
| AOTF bandwidth [nm] | 0.5 - 3 | 1.5 - 6 | 2 - 6 |
| FOV1 [°] | 1.91 x 1.91 | 5.73 x 5.73 | 1.91 x 1.91 |
| FOV2 [°] | 0.2 x 0.2 | 1 x 1 | 1 x 1 |
| Entrance pupil diameter 1 [mm] | 5.24 | 8.72 | 26.17 |
| Entrance pupil diameter 2 [mm] | 50 | 50 | 50 |
| number of pixels | 171 x 171 | 512 x 512 | 171 x 171 |

The optical system consists mainly of aspheric mirrors and of some additional fused silica lenses, resulting in a radiation hard optical system. The conceptual design of the visible channel is shown in Figure 12 with the moveable mirror in the position for stellar occultation observations.

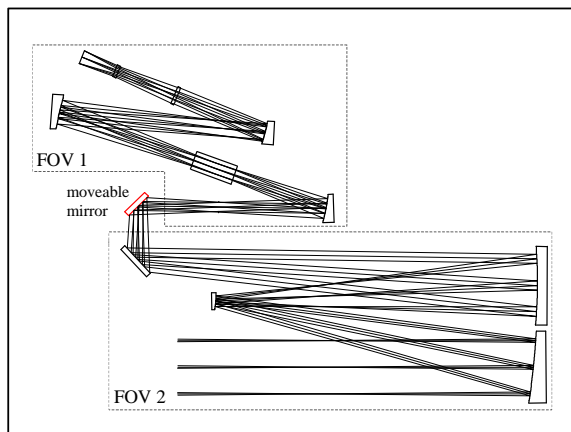


Figure 12: Conceptual optical design of visible channel with the moveable mirror (red) in the stellar occultation position.

The image spotsize, defined as the diameter that encircles 83% of the energy in the PSF, is 1 to 3 detector pixels, depending on the wavelength and the field angle.

A very important issue of the optical system performance is blocking of the zero order of the AOTF. This zero order can be almost completely blocked by placing the AOTF between two crossed polarizers. When the polarizer in front of the AOTF is correctly aligned, the input beam will be diffracted into a 90° rotated output beam which will be transmitted by the polarizer behind the AOTF [16], and the undiffracted beam will be stopped by the second polarizer. Suitable polarizers are Glan-Taylor or Glan-Thompson polarizers. They can have an extinction ratio of 1×10^{-5} or better. To stop the residual unwanted light an aperture stop is placed at the image of the entrance pupil in the back end optics.

6.4. Mechanical structure

The ALTIUS payload is based on a modular concept. The payload will consist of the three different optical channels that can be seen as three modules that are stacked inside the instrument.

Each module is composed of:

- opto-mechanical subunits (supports for the optical parts, holders, brackets);
- electronic boxes;
- a base plate, which supports the brackets of the optical elements, the detectors and the electronics;
- a cover with side panels, which acts also as base plate for the module that is placed on top of this module.

Each module will have its dedicated electronics consisting of detector control electronics, AOTF driver electronics and mechanism control electronics. In case one of the modules would fail, the operation of the other modules is not affected.

The cooling philosophy drives the location of the modules. The NIR detector has its own cooler, cooling it down to 150K. The UV and visible detectors are uncooled. To reduce the dark current noise of these detectors, their temperature must be as low as possible. The UV and VIS detectors are thermally isolated from the rest of their respective module and are thermally coupled with the NIR optical bench. The UV channel module is mounted directly onto the satellite structure, followed by the visible channel module and on top the NIR channel module.

A schematic front view of the payload with the three different channels and apertures for two optical paths per channel is shown in Figure 13.

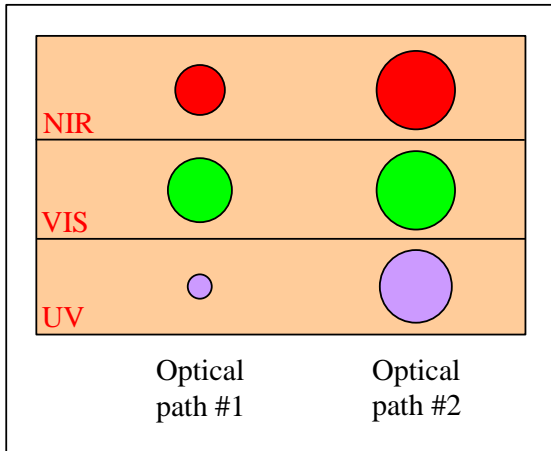


Figure 13: Apertures in payload (front view)

Several mechanisms are needed in the instrument to switch between the different observations modes and to protect the instrument during launch. During launch both apertures of each module should be closed and during operation only one of the two apertures should be open. In solar mode an ND filter and in stellar mode a moveable mirror must be inserted in the optical path.

The aperture covers and the ND-filter are combined in the shutter mechanism. The shutter mechanism, shown in Figure 14, is a slide containing an aperture and a ND-filter. The slide can be placed at three positions:

- during launch and solar occultation observations the aperture of optical path #2 is closed and the ND-filter is behind the aperture of optical path #1
- during stellar occultation observations the aperture of optical path #2 is open and the aperture of optical path #1 is closed
- during bright limb observations the aperture of optical path #2 is closed and the aperture of optical path #1 is open

The different positions in the different modes are shown in Figure 15 and summarized in Table 4, which also gives the position of the moveable mirror. Figure 15 shows a cross section of the shutter mechanism behind the satellite wall.

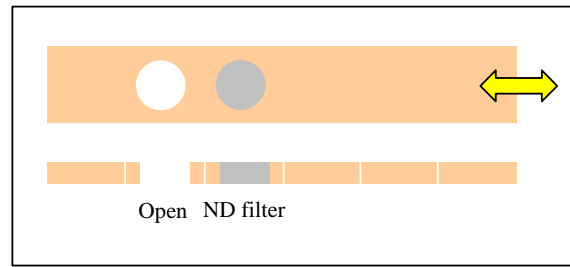


Figure 14: Shutter mechanism (top view + cross section)

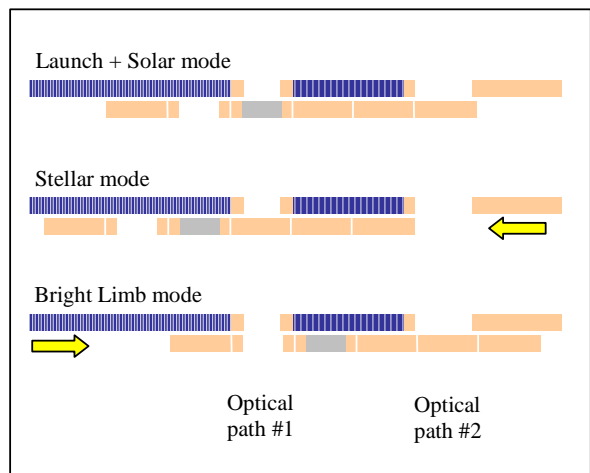


Figure 15: Position of shutter mechanism during the different observation modes (the figure shows a cross section of satellite wall and shutter mechanism)

Table 4: Status of apertures and moveable mirror in the different modes.

| Mode | Optical path #1 | Optical path #2 | Moveable mirror |
|-------------|---------------------|-----------------|---------------------|
| Launch | closed by ND-filter | closed | |
| Bright Limb | open | closed | out of optical path |
| Stellar | closed | open | in optical path |
| Solar | ND-filter | closed | out of optical path |

6.5. Detectors

For the UV and visible channels, a CMOS APS focal plane array from IMEC, Cypress or CMOSIS is envisaged. For the visible channel, the front illuminated version of the detector is chosen. For the UV channel, a thinned back-side illuminated device with additional phosphor coating will be used.

The detector used in the NIR region will be the Neptune SWIR k508 500x256 detector from Sofradir.

7. ALTIUS GROUND SEGMENT

The ALTIUS G/S will be decomposed as follows:

- ALTIUS Mission Operations (AMO), headed by a Mission Operations Manager (MOM), containing the ALTIUS Mission Operations Centre (AMOC) and the ground stations;
- ALTIUS Science and Payload Operations (ASPO), headed by a Project Scientist (Principal Investigator) (PS/PI) and a Science Operations Manager (SOM), containing the ALTIUS Science Operations Centre (ASOC), the ALTIUS Instrument Team, the ALTIUS Mission Scenario Team and the ALTIUS Data Processing Team.

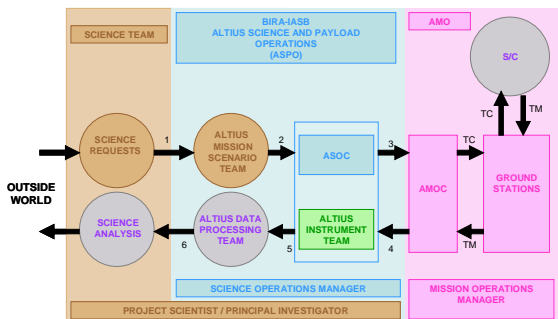


Figure 16: General structure of the ALTIUS ground segment

Figure 17 illustrates the overall AMO. The ALTIUS Mission Operations Centre (AMOC) together with the main ground station (both for telecommanding and telemetry) will be situated in Redu (Belgium). Use of Redu as single G/S is possible thanks to the presence of an isoflux antenna on board the S/C which does not need re-pointing of the S/C for downlinking and hence allows continuous science observations.

As back-up ground station St-Hubert (Canada) is proposed. St-Hubert can also be used as an (occasional) second ground station in case data would be transmitted systematically through the S/C's high gain antenna. In that occurrence the use of only one ground station (in casu Redu) would lead to systematic absence of measurements above a certain region (due to re-pointing of antenna and hence no science observations possible).

The AMOC's Mission Management will plan all routine real-time operations. It will be the interface point with the ASOC.

The EMCS (EGSE and Mission Control System) will execute the pass related activities prepared by the

Mission Management. The EMCS has a nominal and a redundant branch.

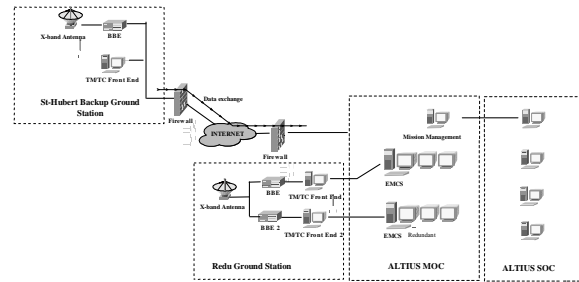


Figure 17: General structure of AMO

The interfaces between the AMOC and the external systems are depicted in more detail in Figure 18.

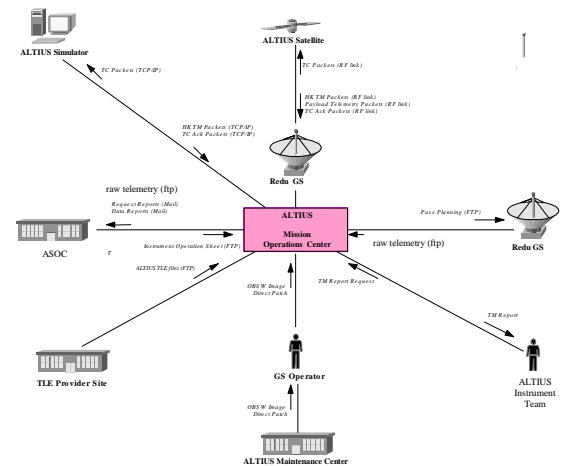


Figure 18: Interfaces to external systems seen from the AMOC

The ASPO building blocks are:

- the Long Term Planning (LTP)
- the Medium Term Planning (MTP)
- the Short Term Planning (STP)
- the Data Ingestion
- the Quick-Look
- the Data Analysis
- the Archive System

The different elements and their interactions are shown in Figure 19.

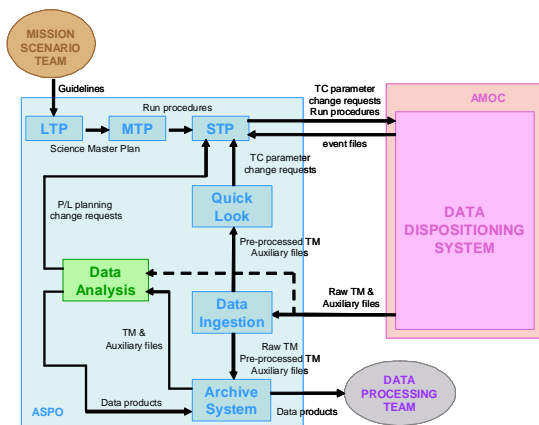


Figure 19: Building blocks of the ASPO

8. CONCLUSIONS

The paper presents a design of an innovative satellite concept that ensures 3-day global coverage of the Earth's atmosphere.

The proposed imaging spectrometer, equipped with an AOTF, fulfils the scientific requirements, and provides a high flexibility for the scientists towards the selection of the spectral bands.

It has been shown that the baseline operational mission can be performed without any limitations using a small platform, based on the PROBA bus. The off-nominal scientific experiments can be executed by the spacecraft, but due to the limitations on the incoming power, a consecutive non-operational orbit should be scheduled to recharge the batteries.

The performant AOCS system combines a high pointing accuracy with a high agility, which is of major importance to support all the identified observation modes.

The mission can be executed using only the Redu ground station, using a 3m X-band antenna. All the obtained science data can be downlinked to the Redu ground station without the need for repointing and interrupting the observations.

In the next phases of the project, the focus shall be placed on:

- Increasing the margins on the power budget
- Increasing the margins on the star tracker blinding
- Detailed payload design
- Investigation of a propulsion system for orbit maintenance and end-of-life disposal

The lead-time for the phase BCD of the ALTIUS mission is about 3.5 year.

9. REFERENCES

- | |
|---|
| [1] McPeters et al., GRL, 27, 2597-2600, [2000] |
| [2] Haley et al. JGR, 109,doi:10.1029/2004JD004588 [2004] |
| [3] Brinkma et al. ACPD, 5, 4893-4928, [2005] |
| [4] Rault, JGR, 110, doi:10.1029/2004JD004970 [2005] |
| [5] von Savigny et al. ACPD, 5, 3701-3722, [2005] |
| [6] Fussen et al. Adv. in Space Res., 35, doi:10.1016/j.asr.2005.04.00, [2005] |
| [7] Gupta and Voloshinov Applied Optics, 43, 2752-2759, [2004] |
| [8] Ross Henderson ALTIUS CDF final report |
| [9] McLinden et al. McLinden, C. A., C. S. Haley, and E. J. Llewellyn (2004), Derivation of polarization from Odin/OSIRIS limb spectra, Geophys. Res. Lett., 31, L20112, doi:10.1029/2004GL020825. |
| [10] Lambert http://www.oma.be/NDSC_SatWG/Documents/SatelliteMissionsPlanning(11Juil2006)_A4.pdf |
| [11] IGACO Report of the Integrated Global Atmospheric Chemistry Observation Theme Team, ESA SP-1282, September 2004 |
| [12] Errera et al. BASCOE Assimilation of Ozone and Nitrogen Dioxide observed by MIPAS and GOMOS: Comparison Between the Two Sets of Analyses, in: ESA Special Publication SP-636: Proceedings of Envisat Symposium 2007, 2007. |
| [13] WMO, 1995: Scientific Assessment of Ozone Depletion: 1994, Global Ozone Research and Monitoring Project. World Meteorological Organization, Geneva, 1995 |
| [14] D.R. Suhre, M. Gottlieb, L.H. Taylor and N.T. Nelamed "Spatial resolution of imaging noncollinear acousto-optic tunable filters", Opt. Eng. 31, 2118-2121 (1992). |
| [15] D.R. Suhre, L.J. Denes and N. Gupta "Telecentric confocal optics for aberration correction of acousto-optic tunable filters", Appl. Opt. 43, 1255-1260 (2004). |
| [16] R.W. Dixon "Acoustic diffraction of light in anisotropic media", IEEE J. Quantum Electr., QE-3, 85-93 (1967) |